



Clean manufacturing of cellulose nanopapers by incorporating lignin and xylan as sustainable additives

Sergejs Beluns^a, Sergejs Gaidukovs^{a,*}, Oskars Platnieks^a, Anda Barkane^a, Gerda Gaidukova^b, Līga Grase^c, Martins Nabels-Sneiders^a, Andrejs Kovalovs^d, Vijay Kumar Thakur^{e,f,a}

^a Faculty of Materials Science and Applied Chemistry, Institute of Polymer Materials, Riga Technical University, P.Valdena 3/7, LV-1048, Riga, Latvia

^b Faculty of Materials Science and Applied Chemistry, Institute of Applied Chemistry, Riga Technical University, P.Valdena 3/7, LV-1048, Riga, Latvia

^c Faculty of Materials Science and Applied Chemistry, Institute of Materials and Surface Engineering, P.Valdena 3, LV-1048, Riga, Latvia

^d Institute of Materials and Structures, Riga Technical University, 6b Kipsalas St., 1048 Riga, Latvia

^e Biorefining and Advanced Materials Research Center, Scotland's Rural College (SRUC), Kings Buildings, West Mains Road, Edinburgh EH9 3JG, U.K.

^f School of Engineering, University of Petroleum & Energy Studies (UPES), Dehradun 248007, Uttarakhand, India

ARTICLE INFO

Keywords:

Nanofibrillated cellulose
Mechanical properties
Green modification
Forestry residue
Food packaging

ABSTRACT

In this work, we report for the first time the clean manufacturing of cellulose nanopapers by a green path of mixing nanocellulose suspension in water with lignin and xylan. The procedure involves grinding the old wastepaper, microfluidizing, casting, and water evaporation. The introduction of lignin and xylan with various loadings from 1 to 30 wt% showed that properties could be significantly tuned. Moreover, lignin and xylan loadings introduced into these nanopapers endow them with improved mechanical and structural properties, as evidenced by tensile tests and scanning electron microscopy analysis (SEM). Xylan strongly promotes the transparency of nanopapers. Even at low loadings, the addition of xylan and lignin enhanced specific strength by 1.3-fold, while specific elastic modulus was found to exhibit a 2-fold enhancement. Mathematical modeling complemented the analysis of tensile properties. Thermogravimetric analysis testified that the wastepaper is made of highly purified cellulose. Furthermore, thermal properties analysis shows that the modified nanopapers have higher thermal conductivity and diffusivity than the unmodified ones. Thermal conductivity was found to improve 3.5-fold for compositions with 30 wt% loading of modifiers corresponding to the developed denser structure as revealed by SEM. The introduced crosscut and surface structure changes enable functional applications to obtain packaging, filtering, biomedical, and sensor materials.

1. Introduction

Mimicking the unique biomechanical properties of plants and trees (Liu et al., 2021; Tedeschi et al., 2020) in complex systems is an emerging direction for advanced cellulose materials (Markstedt et al., 2019; Sun et al., 2020; C. Zhang et al., 2020). Authors have so far focused on studying the effect of the chemical pretreatment to explore the synergic properties of lignocellulose fibers. Unfortunately, most pretreatments eliminate hemicellulose, thus leading to a relatively limited amount of research that evaluates hemicellulose's contribution (Bashar et al., 2019; Filipova et al., 2020; Xiao et al., 2015; K. Zhang et al., 2016). Controlling the amount of lignin with pretreatment is relatively complicated and extremely depends on the source of lignocellulose, thus creating issues with repeatability. In the present

investigation, our scope is to borrow concepts from nature and implement them in cellulose-based materials, i.e., nanopapers.

Studies on various lignocellulose polymers indicate that xylan (hemicellulose) and lignin can increase nanopaper's performance compared to pure cellulose fibers (Abdulkhani et al., 2020; Taylor et al., 2020). Xylan binds long cellulose fibers together, leading to increasing entanglement and ultimately improving the paper's mechanical properties (Grantham et al., 2017; Naidu et al., 2018). Berglund et al. showed that the compression properties of bacterial cellulose hydrogels saw an increase in elastic modulus with the addition of glucomannan, while xylan improved elongation at break (Berglund et al., 2020). In contrast, Tedeschi et al. report hydrolyzed lignin's effect on xylan–cellulose bioplastics (Tedeschi et al., 2020) and demonstrated that it enhances hydrophobicity, water vapor, oxygen, and grease barrier properties.

* Corresponding author.

E-mail address: sergejs.gaidukovs@rtu.lv (S. Gaidukovs).

<https://doi.org/10.1016/j.carpta.2022.100207>

Received 17 December 2021; Received in revised form 3 April 2022; Accepted 15 April 2022

Available online 17 April 2022

2666-8939/© 2022 The Authors. Published by Elsevier Ltd. This is an open access article under the CC BY-NC-ND license (<http://creativecommons.org/licenses/by-nc-nd/4.0/>).

Lignin has been shown to reduce the impact of UV irradiation and microbial attacks on cellulose, and it can form a hydrophobic protective layer that prevents cellulose swelling (Ibrahim et al., 2019; Martínez et al., 2005). In addition, lignin increases the thermal stability of nanofibrillated cellulose materials (NFC) (Watkins et al., 2015; N. Zhang et al., 2019).

Two significant performance factors have motivated us for the selection of lignin and xylan to modify cellulose nanopapers to improve the existing material solution. The first factor is the possibility of controlling the material's durability (resistance to UV-light and moisture). The second is the usage of natural biobased modifiers to tune up the necessary tensile and thermal characteristics. At the same time, the material will remain biodegradable, and the released degradation products will be without concern for human health and the environment. In this direction, the combination of these three key biopolymers has remained unexplored in hybrid compositions, which could be applied to further tune and control the properties of nanopapers (NPs).

The effects of lignin and xylan combinations, i.e., hybrid modifiers, on cellulose nanopaper performance have been investigated in this study. The contribution of modifiers to the assembly of NFC networks has been adjusted with different interaction mechanisms of lignin and xylan. Mathematical modeling based on experimental data characterized the hybrid composition potential. Sourcing lignocellulose biopolymers from cheap waste material resources have emerged as a sustainable solution (Agate et al., 2020; Kumar et al., 2020; Rajinipriya et al., 2018) to implement in a circular economy (Machado et al., 2020). Waste usage in nanopaper manufacturing provides a viable economic route for creating value-added cellulose products and is of particular interest to the packaging industry. Therefore, the specific objective of this work has been to develop a series of cellulose nanopapers containing only natural modifiers and recycled waste paper through a clean manufacturing processing route. These materials could be used as packaging materials for food, vegetables, and fruits adapted for filtering and purification processes and integrated into various sensors.

2. Materials and methods

2.1. Materials

The old, unutilized laboratory filter paper waste was used as a cellulose source. Before processing, it was dried at 60°C overnight. Wastepaper was ground with the Retsch cutting mill SM300, with a sieve size of 0.25 mm. The mill was fed manually, and the rotation speed was kept at 1500 rpm. The milled paper was used without further purification and treatment. Deionized (DI) water was used for aqueous dispersion preparation. Kraft lignin and beechwood xylan were obtained from Aldrich. They were used as received without additional processing. Laboratory-grade sodium hydroxide (NaOH) was used for lignin suspension preparation without further purification.

2.2. Cellulose nanofibrils processing

Nanofibrillated cellulose (NFC) was prepared by dispersing 1 wt% of milled paper in DI water. The obtained aqueous dispersion was mixed in an ordinary kitchen blender (800W) and then passed through a microfluidizer (LM20, Microfluidic, U.S.A.) equipped with a chamber H210Z (200 µm). Five passes were used to increase the degree of defibrillation. The pump pressure was set at 30 000 psi.

2.3. Cellulose nanopapers preparation

50 g of kraft lignin was first suspended in 470 mL of DI water and stirred magnetically for 1 h at 85°C. The suspension was stabilized to pH 10 using a strong alkaline solution (NaOH). A dark, homogeneous suspension was obtained, having a lignin concentration of 10 wt% (adjusted with evaporation).

30 g of beechwood xylan was dissolved in 285 mL of DI water and stirred magnetically at 80–85°C for 1 h until the xylan dissolved in the water. A slightly brown, viscous solution was obtained, having a xylan concentration of 10 wt% (adjusted with evaporation). After cooling at room temperature, both solutions were used as follows in the preparation of the samples.

Nanopaper films were produced by casting 1 wt% dispersion onto polystyrene (PS) Petri dishes. Dispersions and solutions were mixed (with xylan and lignin) to selected concentrations, magnetically stirred for 2 h, cast onto prepared Petri dishes, and placed at room temperature until evaporation. Afterward, the nanopaper films were dried in a laboratory oven at 50°C for 24 h. 1, 2.5, 5, 10, 20, 30 wt% of lignin (L) and xylan (X) loadings into cellulose nanopaper were prepared. In the text, single filler samples have been abbreviated as L and X, combined with the filler concentration number. At the same time, several complex compositions with simultaneous lignin and xylan loading were also proposed, abbreviated as LX systems. For example, the X1 sample corresponds to xylan 1 wt% loading, L1 sample – lignin 1 wt% loading, L1X1 sample – lignin 1 wt% and xylan 1 wt% complex loadings. A sample without any loading is abbreviated as cellulose nanopaper (CNP). 19 modified nanopapers and 1 reference (CNP) sample were prepared and characterized.

2.4. Thermal characterization

The thermal stability was evaluated with thermogravimetric analysis (TGA) using a Mettler TG50 instrument. Measurements were performed on samples with a weight of about 10 mg. Heating under an oxygen atmosphere was conducted from 25 to 750°C with a heating rate of 10°C/min.

The thermal conductivity and thermal diffusivity were evaluated with the Netzch LFA 447 NanoFlash System. The film specimens were heated with a Xenon flash lamp (10 J/pulse) in the air. The measurements were taken at three temperatures: 25°C, 35°C, and 45°C. Before testing, the samples were coated with graphite to enhance the absorption of light energy and the emission of infra-red radiation to the detector.

2.5. Morphology

The FEI Nova NanoSEM 650 Schottky field emission scanning electron microscope (FESEM) was used to examine the structure of NFC and NPs. The morphology of nanopapers was studied with Scanning Electron Microscopy (SEM) at a voltage of 1 kV. Crosscuts were obtained in liquid nitrogen. Coatings were not applied on the surface or crosscut surfaces. To get images of NFC, Scanning Transmission Electron Microscopy (STEM) probe was used. Measurements were performed in transmission configuration using an acceleration voltage of 10 kV. A 400 W ultrasound probe was used to sonicate a diluted NFC suspension for 1 minute. After that, the NFC suspension droplet was placed on a copper grid (mesh 200) and allowed to evaporate at room temperature.

2.6. Mechanical properties

Tensile tests were performed on nanopaper films using a universal testing machine, Tinius Olsen model 25ST (USA), equipped with a load cell of 5 kN at 1 mm/min crosshead speed. Cellulose nanopaper was cut into a rectangle strip of 10 mm in width and about 40 mm in length. The Gage length between grips was 20 mm. Five parallel measurements were performed for each film sample at room temperature and ambient conditions. The samples were conditioned for 48 h at 50% humidity and measured at 20°C.

2.7. Experimental Design and Response Surface Technique

The effect of lignin and xylan on the mechanical properties of the

nanopaper was assessed in several stages: (a) the selection of the design parameters and their intervals of variation, (b) the development of the design experiment for the parameters selected, (c) experimental testing, and (d) the determination of the second-order polynomial regression equation.

The full-factorial design (FFD) has been selected, and it generated 9 experimental runs for two parameters and three levels (Figures S1). The minimum and maximum levels for the design parameters are given in Table 1.

A second-order polynomial regression Eq. (1) has been proposed to predict the response of polymer composites.

$$F(x) = b_0 + \sum_{i=1}^m b_i x_i + \sum_{i=1}^m \sum_{j=1}^m b_{ij} x_i^2 + \sum_{i=1}^m \sum_{j=1}^m b_{ij} x_i x_j \quad (1)$$

where $F(x)$ is the response, x_i and x_j are the values of parameters, b_0 is the constant, b_i , b_j , and b_{ij} are regression coefficients, respectively, and m is the number of the parameters.

The design parameters and experimental values of specific modulus, specific stress, and strain were determined by averaging the test results of 5 specimens of nanopapers and are presented in the supplementary information.

3. Results and discussion

3.1. Morphological properties

After shredding in the mill, the mean length of fibers was 280 μm , and the width was up to 50 μm . Therefore, mechanical delamination with microfluidization was carried out to reduce the fiber dimensions to the nanoscale. STEM micrograph shows long nanofibrils (Fig. 1), with an average width of 86 ± 41 nm.

Fig. 2 presents the surface and cross-section micrographs of the obtained NPs. The network of randomly orientated fibers is visible with dimensions in micrometers, indicating that NFC has formed microfibril aggregates. Similar observations were made by Henriksson et al. (Henriksson et al., 2008). In addition, a crosscut image of NP shows a rough structure with visible microfibril ends. The addition of lignin to NFC significantly changes the crosscutting structure of NPs, introducing visible voids in all examined samples. Lignin addition also reduces crosscut surface roughness. The L5 sample has larger voids than the L1. Thus, the addition of lignin directly causes the formation of voids, as observed in the microstructure. While the construction of cavities could be helpful in specific filtration applications, it would directly influence the mechanical properties of the present NPs (Hanhikoski et al., 2020; Robles et al., 2021).

The addition of xylan has been found to contribute to the formation of a relatively smooth crosscut surface, like the surface formed by CNP. The X1 sample shows some structural defects, such as voids and layer separation, which are not visible in the X5 sample. As a result, xylan fills the void spaces between cellulose fibrils, resulting in continuous smooth crosscut surfaces with no visible micro- or nanostructure voids. As reported by Goksu et al. (Goksu et al., 2007) and Hansen et al. (Hansen et al., 2012), xylan content can significantly affect the porosity and, therefore, water vapor transmission rate. Hybrid compositions L1X1 and L5X5 show that lignin strongly influenced the formation of the structure, which is visually comparable to L1 and L5 NPs.

The transparency and visual appearance of NPs are presented in Fig. 3. The reference CNP shows a distinct white color without

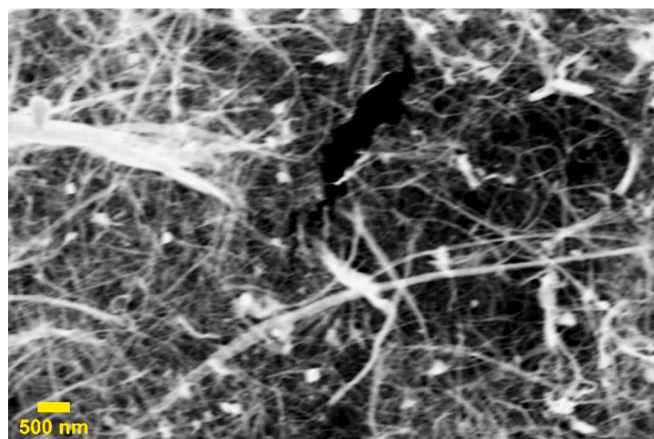


Fig. 1. STEM image of NFC obtained from wastepaper.

transparency. The addition of lignin results in a substantial color shift from yellow to dark brown and the appearance of grainy texture in the form of small lignin particle agglomerates. At the same time, all xylan NPs are transparent, but loadings of 2.5 wt% and above yield a yellowish tint in color. It has been reported earlier that eliminating structural cavities in nanopapers yield transparent structures due to the significantly reduced light scattering (Isobe et al., 2018). In our case, casting did not yield such a dense structure for CNP. Still, as revealed by SEM analysis, xylan fills all the cavities between cellulose fibrils, thus providing a simple modification route for transparent NP.

3.2. Tensile properties

The stress-strain curves measured for NPs samples are presented in Fig. 4. The behavior of all curves is predominantly linear, consisting of the elastic and plastic regions. A substantial increase in the samples' rigidity and material brittleness for lignin, xylan (loadings above 5 wt %), single, and complex filling systems has been observed. It has been suggested that such behavior is caused by decreased slippage yield deformation between the extended cellulose fibrils rather than by covalent bond breakage (Hubbe et al., 2017).

The characteristic tensile properties of elastic modulus, tensile strength, and strain have been summarized to compare single lignin and xylan fillers in Fig. 5. Their hybrid materials (LX) are outlined as surface charts in Fig. 6. Both lignin and xylan reveal that the addition of L2.5 and X2.5 contents produces a substantial increase in specific elastic modulus, but xylan also contributed to increased specific strength values (Fig. 5). At and above 5 wt% lignin loadings, samples show lower specific modulus values than neat CNP. 2.5% addition of Lignin and xylan to NPs showed a 2-fold increase and 1.8-fold increase for specific elastic modulus values. An increase in specific tensile strength was measured for the X2.5 and X5 samples, indicating a 1.3-fold increase compared to CNP.

In addition, all four xylan compositions with loadings up to 10 wt% showed high specific modulus values, but further addition of xylan resulted in a drop for specific modulus values. The increase in tensile strength and elastic modulus could be explained by growth in the contact surface between fibrils, a decrease in voids, and overall porosity values, forming more hydrogen bonds and dense structures. Relatively shorter and more branched xylan molecules act as surface modifiers by increasing entanglement between NFC; thus, slippage between fibers during deformation is more complicated (Liu et al., 2021). Increasing xylan content could yield phase separation between NFC as local agglomerates of cellulose nanoparticles are formed and evidenced by SEM (Linder et al., 2003). These more soft xylan phase sections pose significantly lower mechanical strength, weaken overall composite film, and explain the poor mechanical performance observed for X10, X20, and

Table 1

Process parameters and their levels

Parameters	Levels		
Lignin (wt%)	1	2.5	5
Xylan (wt%)	1	2.5	5

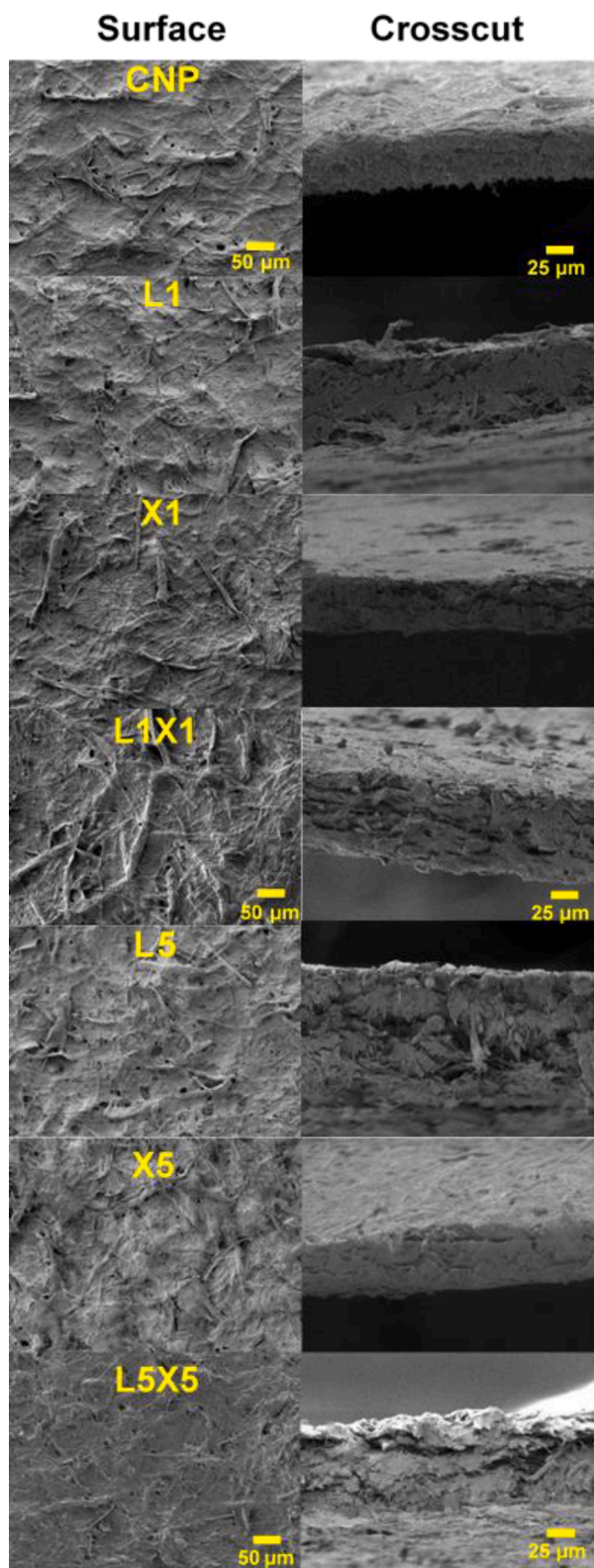


Fig. 2. SEM images of cellulose nanopapers surfaces and crosscuts with lignin and xylan loadings.

X30 samples. Lignin-modified NPs saw decreased specific strength values for all concentrations. This could be defined by introducing voids and structural defects observed in SEM images (Fig. 2). While, higher lignin particles concentrations similarly saw a further decrease as large particles developed voids and defects in the structure, which does not

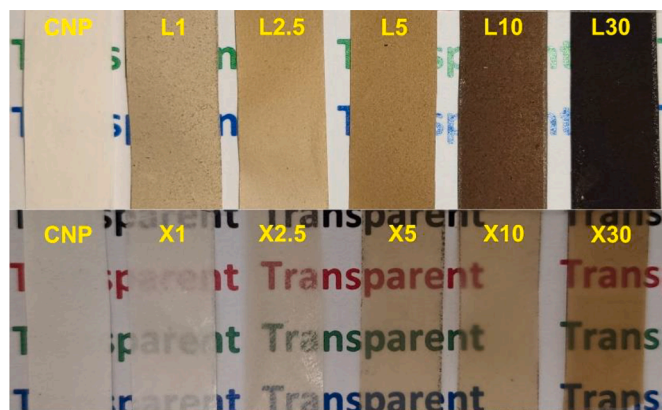


Fig. 3. Transparency comparison of prepared NPs with lignin and xylan.

pose high mechanical properties. Elongation at the break for xylan samples with loading up to 5 wt% remained comparable to CNP, while higher concentrations saw decreased values. All lignin concentrations showed a significant decrease in strain values from 3% to around 1% compared to CNP. The decline in elongation values is visible in a shorter plastic region, indicating that some compositions promoted fibril slippage.

Considering hybrid compositions, an in-depth comparison can be made for tensile properties. Using the experimental data as a basis, a response surface plot was constructed for each tensile characteristic to model component contributions (Table S1). The experimental data obtained in testing were used to construct the second-order polynomial regression equation using the program EdaOpt (Auzins et al., 2014). The relationships between the design variables $x_i = (X_1, X_2)$ and the corresponding behavior functions Y_i are given as follows:

Specific modulus:

$$YSM = 3273 + 277 \cdot X_1 + 555 \cdot X_2 - 84 \cdot X_1 \cdot X_1 - 94 \cdot X_2 \cdot X_2 - 75 \cdot X_1 \cdot X_2, \quad (2)$$

Specific strength:

$$YSS = 64.63 - 18.19 \cdot X_1 + 10.75 \cdot X_2 + 1.83 \cdot X_1 \cdot X_1 - 1.98 \cdot X_2 \cdot X_2 - 0.247 \cdot X_1 \cdot X_2, \quad (3)$$

Strain:

$$YS = 2.939 - 0.987 \cdot X_1 + 0.02 \cdot X_2 + 0.1147 \cdot X_1 \cdot X_1 - 0.0213 \cdot X_2 \cdot X_2 + 0.04 \cdot X_1 \cdot X_2, \quad (4)$$

where X_1 and X_2 are the weight contents of the Lignin and Xylan, respectively.

Specific elastic modulus, specific tensile strength, and strain graphs (Fig. 6) show the highest mechanical performance for samples modified with xylan from 2.5 to 5.0 wt% and up to 2.5 wt% added lignin. Surface charts also indicate that up to 1.0 wt% lignin can be added to retain relatively high specific strength and strain values, as other sections discuss the benefits of adding lignin. The strain at break values dropped strongly for hybrid compositions due to the lignin particles' impact on the structure. The optimal specific strength values were obtained for composition L2.5X2.5, which combines the cellulose surface modification and densification by xylan, negating the formation of voids in the structure induced by adding lignin particles. Compared to single filler systems, the creation of bio-based hybrid compositions has been shown in the literature to obtain improved mechanical qualities in the fiber-fiber and fiber-particle compositions (Atmakuri et al., 2020; Nunna et al., 2012). In our situation, the specific elastic modulus was the only mechanical characteristic that improved from hybrid compositions containing 2.5 wt% xylan and lignin loadings.

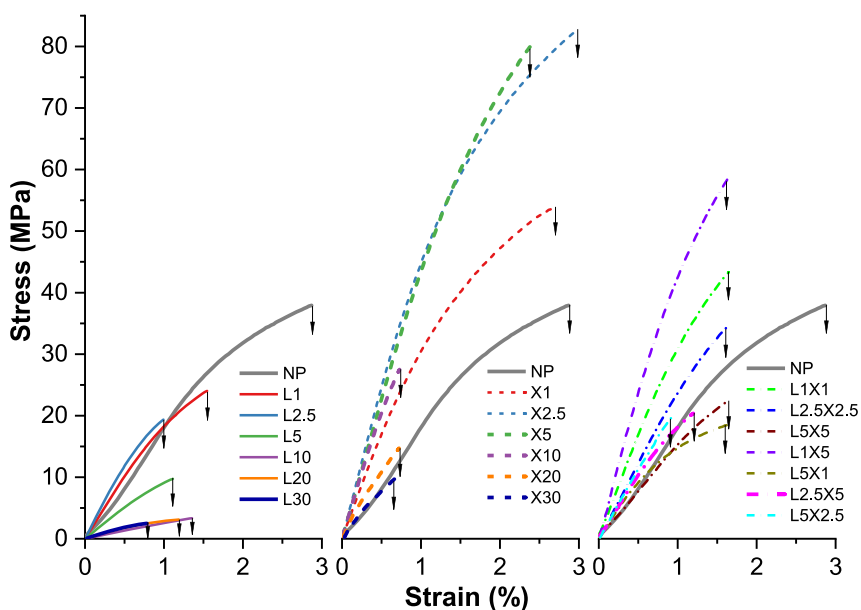


Fig. 4. Tensile curves of nanopapers.

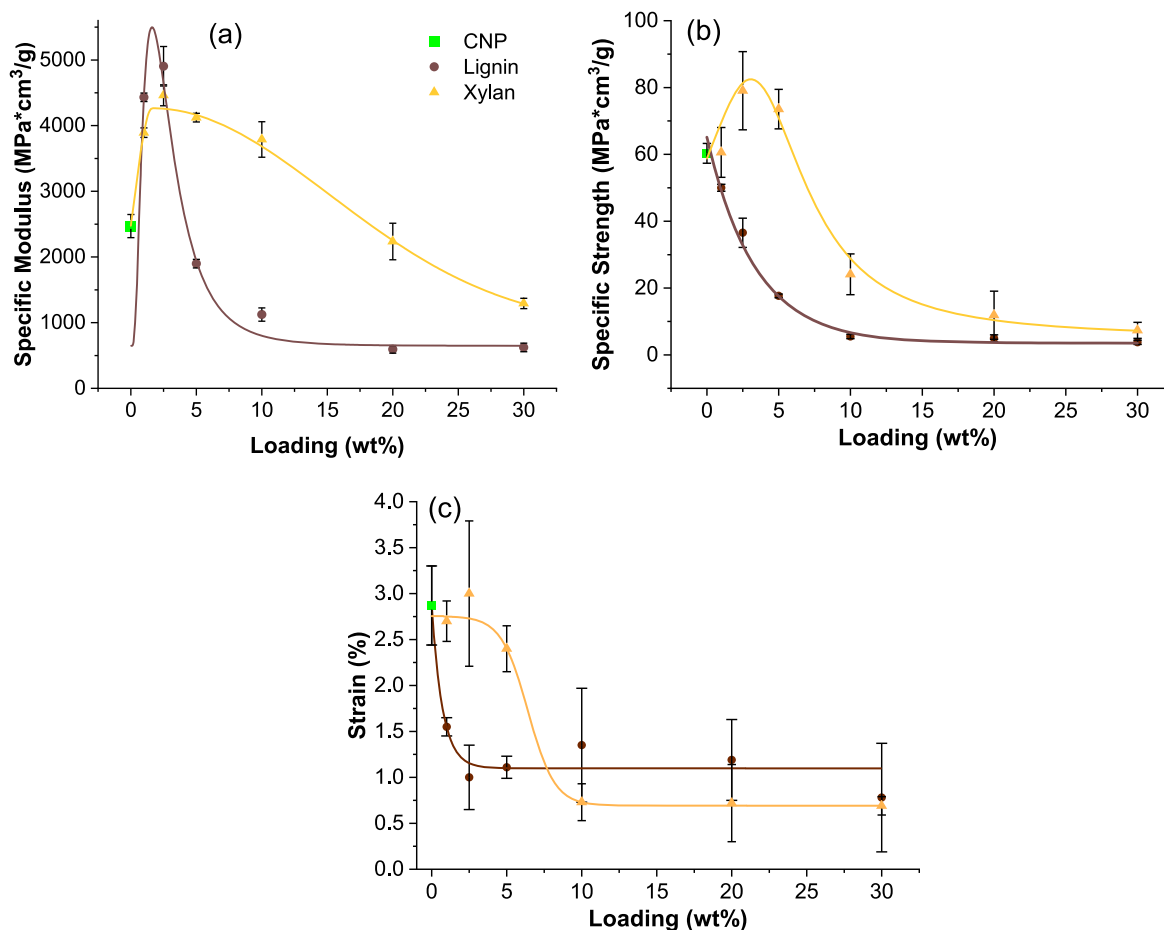


Fig. 5. Tensile properties of cellulose nanopapers: specific elastic modulus (a), specific strength (b), and strain (c).

3.3. Thermooxidative stability

Thermooxidative stability of the nanopaper and its composites was determined using thermogravimetric analysis (TGA) with a heating rate

of 10°C /min under an oxidative air atmosphere. TGA and derivative weight loss of the prepared nanopaper composites have been shown in Fig. 7 (a) and (b), respectively.

Lignin is known for its superior thermal stability over other cellulose-

appears to be the highest (526°C). The observations in Fig. 7 (b) and Table 2, where the highest T_{max} is 327°C for CNP, align with the literature (Mtibe et al., 2015; Sethi et al., 2019).

The weight loss for all samples starts with the evaporation of adsorbed water, and the temperature range up to 200°C is commonly attributed to this process (Brillard et al., 2017; N. Zhang et al., 2019). Depending on sample composition, the adsorbed water amount has been from 4 to 10 wt%. This phenomenon could be attributed to an additional covalent linkage between lignin and cellulose fibrils (Mahendra et al., 2019) that bind with -OH groups; the same goes for xylan. Therefore, less water is absorbed. Thus, xylan and lignin introduction has reduced the hydrophilicity of the NPs and has increased the initial thermal stability.

Reportedly the primary degradation of NFC happens from 206 to 381°C when adsorbed water has already been evaporated (Isaac et al., 2018; N. Zhang et al., 2019). The cellulose pyrolysis model says that cellulose melts at a range of 200 to 280°C, and then the formation of dehydrogenated cellulose happens, followed by strong cellulose depolymerization (Isaac et al., 2018; N. Zhang et al., 2019). Fig. 7 shows similar three-step thermal degradation of the CNP, heating to 200°C removes adsorbed water, then approximately up to 330°C next steps of cellulose melting and dehydrogenation occur, followed by strong depolymerization, leaving around 20 wt% of the sample left. Thermal degradation after 330°C appears almost as a separate degradation step, not reported when an inert nitrogen atmosphere is used (N. Zhang et al., 2019). This leads to a much lower char yield of the NPs due to thermal oxidation of the char in the range of 440 to 580°C (Shen et al., 2013). The addition of L and X decreases maximum degradation temperature (thermal stability) by 29, 47, 28, 2, and 31°C for L1, L10, X1, X10, and L5X5 composites respect. Changes in structure affected moisture absorption and significantly contributed to observed differences. L10 composition with a remaining 50 wt% showed superior thermal stability. Table 2 shows that lignin addition increases char yield by 1 and 22 wt% for L1 and L10 composites.

3.4. Thermal conductivity

Table 3 summarizes NPs density, diffusivity, activation energy (E_a), and inherent conductivity value (λ_0). It has been proposed that the pore size in NPs is too small for air to participate in heat conduction; thus, cellulose crystal orientation and interfacial bonding strength play a significant role in thermal conductivity parameters (Diaz et al., 2014; Uetani & Hatori, 2017). The film casting process resulted in non-aligned NPs, eliminating anisotropy for thermal properties. The formation of interfaces can be expected from the density of prepared NPs (Table 3). The addition of 1 wt% lignin decreased density to 0.48 (g/cm³), the lowest value observed from prepared NPs.

While the loading of more lignin increased density value, they remained comparable to CNP. As discussed in the morphology section, lignin resulted in various defects like voids, which contributed to higher porosity and lower density values. While, as proposed before, xylan is a shorter, more branched molecule that can fill gaps between NFC networks and increase interfacial bonding, this is reflected as a loss of

Table 2
Thermal degradation characteristics of cellulose nanopapers.

Sample	Onset degradation temp. (°C)	Maximum degradation temp. (°C)	Char yield (wt%)
CNP	268	327	0
L	182	414	20
X	207	251	7
L1	154	298	3
L10	176	280	24
X1	225	299	3
X10	198	325	3
L5X5	188	296	24

Table 3

Density, diffusivity (at 25°C), specific heat (at 25°C), activation energy E_a and inherent conductivity value λ_0 of cellulose nanopapers.

Sample	Bulk density (g/cm ³)	Diffusivity (mm ² /s)	λ_0 (W/(m·K))	E_a (kJ/mol)
CNP	0.63 ± 0.06	0.091	0.27	3.59
L1	0.48 ± 0.03	0.096	0.22	3.61
L2.5	0.52 ± 0.03	-	-	-
L5	0.55 ± 0.03	-	-	-
L10	0.61 ± 0.05	0.167	0.42	4.01
L20	0.63 ± 0.04	-	-	-
L30	0.66 ± 0.07	0.142	0.22	1.89
X1	0.89 ± 0.06	0.099	0.51	2.64
X2.5	1.05 ± 0.04	-	-	-
X5	1.09 ± 0.03	-	-	-
X10	1.14 ± 0.04	0.180	2.73	6.81
X20	1.24 ± 0.04	-	-	-
X30	1.36 ± 0.03	0.161	1.16	3.93
L1X1	0.64 ± 0.04	0.076	0.50	5.54
L1X5	1.01 ± 0.04	-	-	-
L5X1	0.6 ± 0.03	-	-	-
L2.5X2.5	0.69 ± 0.05	-	-	-
L2.5X5	0.99 ± 0.02	-	-	-
L5X2.5	0.79 ± 0.04	-	-	-
L5X5	0.89 ± 0.03	0.103	0.49	4.90

porous structure (Fig. 2) and significantly increased density in range from 0.89 to 1.36 (g/cm³) showing 1.4 to 2.2-fold increase compared to CNP. The changes in thermal conductivity coincide with density changes (Fig. 8), as NPs with higher density show higher values. The L10 sample and L30 samples show slight deviation from predicted changes. Two conflicting effects could explain it. The formation of larger irregular voids reduces density. Lignin particle packing between NFC fibrils enhances thermal conductivity. The addition of xylan has been found to show around a 3 to 4-fold increase in thermal conductivity, while even high loadings of lignin did not exceed a 2-fold increase. The L1 sample showed the lowest thermal conductivity between NPs in all measured temperatures. Hybrid compositions inherited thermal properties identical to samples modified only with lignin. This indicates that lignin intervenes with xylan dispersion and the formation of interfacial bonding. Thermal conductivity slightly increased when measurements were performed at a higher temperature. This is commonly explained by the rise in phonon conduction for solids that are not metals.

Thermal diffusivity changes can be attributed to adsorbed water content, indicated by TGA (Fig. 7), and chemical groups on fiber surface

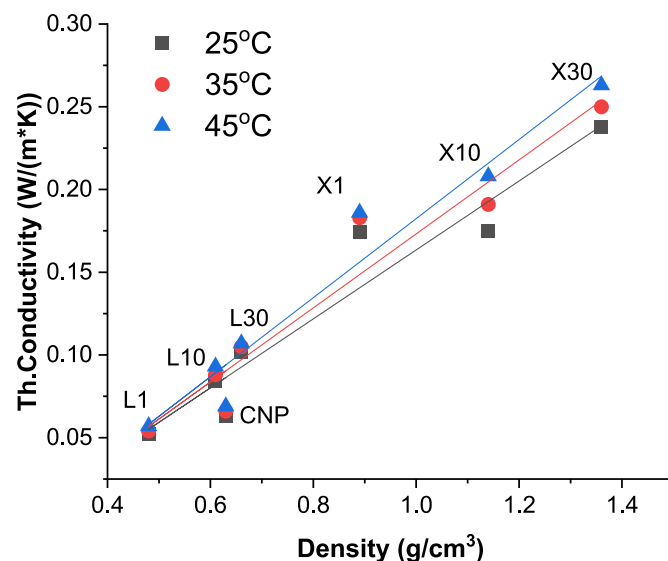


Fig. 8. Thermal conductivity vs. bulk density of cellulose (CNP), lignin (L), and xylan (X) nanopapers.

(Wang et al., 2021). Thus, it can be assumed that branched hydrophilic xylan molecules would promote water adsorption compared to more hydrophobic lignin. This is reflected in Table 3, where all compositions based on xylan show a significant increase in diffusivity values. The best comparison can be made with X1 and L1 samples, where xylan NP shows a 2-fold increase and lignin NP shows almost no change in thermal diffusivity compared to CPN. The high content of modifiers introduces various structural defects that negate the water adsorption effect, and surface groups strongly influence thermal diffusivity. This could explain a significant increase in diffusivity values for L10 and X10 NPs.

In contrast, a subsequent decrease in values for X30 and L30 NPs could be attributed to substantial structural changes in NPs. Thermal diffusivity did not show strong temperature dependence. The X10 and X30 NPs samples' thermal conductivity could be attributed to the formation of separate (new) phases in higher concentrations, while X1 xylan acts more as a cellulose surface modification agent.

Fig. 9 was used to determine E_a values utilizing the slope of the approximate straight lines in the Arrhenius plot. While λ_0 was calculated from the Arrhenius equation, using the method described in (Gaidukovs et al., 2018). The activation energy indicates the role of distributed nanoparticles in NPs for insulation properties of composite as another layer is added that blocks or promotes heat transfer, and an electric current is created (Bertasius et al., 2020). Thus, λ_0 and E_a values depend on the nanoparticle's nature or formed agglomerates or layers in case of high loadings. Table 3 indicates a 1.9-fold decrease of activation energy was achieved for the L30 sample, while X10 saw a 1.9-fold increase. E_a did not show a strong correlation with thermal conductivity, but this can be explained by significantly altered microstructure. Most of the sample's activation energy increased similarly to thermal conductivity and diffusivity. Lignin compositions showed either negative trends or similar results to CNPs.

4. Conclusions

Wastepaper has huge potential to be an excellent source for nanopaper production and fits the circular economy goals. Water suspensions have a significant advantage over other studies implementing various organic solvents. Using lignin and xylan solutions for nanopapers shows multiple benefits as they act more as surface modification agents. Their high loadings prove to be disadvantageous due to phase separation and the heterogeneous structure of these nanopapers. Lignin introduces defects and heterogeneous elements, while xylan fills gaps between cellulose fibrils to create a more homogenous system. The structural changes induced by adding xylan reduce light scattering and yield transparent nanopaper. Defects caused by lignin remain in the structure, while xylan seems to lower the size of formed voids and isolate them. The use of lignin can increase stiffness, resulting in decreased tensile strength and elongation values. The densification of the structure leads to an increase in thermal conductivity. The obtained nanopaper with tunable morphology has shown great perspectives as packaging materials and filters. They would also benefit from developing clean manufacturing routes from waste sources.

CRedit authorship contribution statement

Sergejs Beluns: Visualization, Investigation, Formal analysis, Writing – original draft. **Sergejs Gaidukovs:** Conceptualization, Methodology, Writing – review & editing, Supervision. **Oskars Platnieks:** Formal analysis, Writing – review & editing. **Anda Barkane:** Formal analysis. **Gerda Gaidukova:** Resources. **Liga Grase:** Resources. **Martins Nabels-Sneiders:** . **Andrejs Kovalovs:** Software, Formal analysis. **Vijay Kumar Thakur:** Writing – review & editing.

Declaration of Competing interests

The authors declare that they have no known competing financial

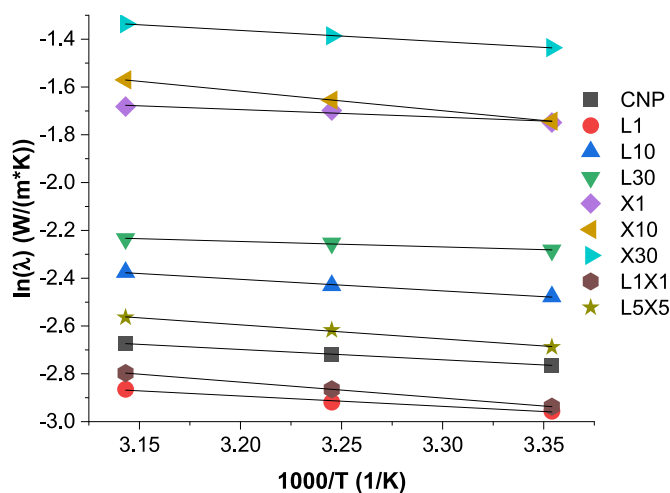


Fig. 9. Arrhenius plot: dependence of thermal conductivity on temperature for cellulose (CNP), lignin (L), xylan (X), and hybrid (LX) nanopapers.

interests or personal relationships that could have appeared to influence the work reported in this paper.

Acknowledgments

This research is funded by the Latvian Council of Science, project RealHLC, project no. lzp-2019/1-0390. This research is funded by the Riga Technical university PhD grant, Development of scientific activity in universities, DOK.PMI/20, Performance funding for doctoral grant MLKF.

Supplementary materials

Supplementary material associated with this article can be found, in the online version, at [doi:10.1016/j.carpta.2022.100207](https://doi.org/10.1016/j.carpta.2022.100207).

References

- Abdulkhani, A., Najd Mazhar, A., Hedjazi, S., & Hamzeh, Y. (2020). Preparation of xylan bio-composite films reinforced with oxidized carboxymethyl cellulose and nanocellulose. *Polymer Bulletin*, 77(12), 6227–6239.
- Agate, S., Tyagi, P., Naithani, V., Lucia, L., & Pal, L. (2020). Innovating generation of nanocellulose from industrial hemp by dual asymmetric centrifugation. *ACS Sustainable Chemistry & Engineering*, 8(4), 1850–1858.
- Atmakuri, A., Palevicius, A., Vilkauskas, A., & Janusas, G. (2020). Review of hybrid fiber based composites with nano particles—material properties and applications. *Polymers*, 12(9), 2088.
- Auzins, J., Janushevskis, A., Janushevskis, J., & Skukis, E. (2014). Software EDAOpt for experimental design, analysis and multiobjective robust optimization. In *OPT-i 2014 - 1st International Conference on Engineering and Applied Sciences Optimization, Proceedings* (pp. 1055–1077).
- Bashar, M. M., Zhu, H., Yamamoto, S., & Mitsuishi, M. (2019). Highly carboxylated and crystalline cellulose nanocrystals from jute fiber by facile ammonium persulfate oxidation. *Cellulose*, 26(6), 3671–3684.
- Berglund, J., Mikkelsen, D., Flanagan, B. M., Dhital, S., Gaunitz, S., Henriksson, G., et al. (2020). Wood hemicelluloses exert distinct biomechanical contributions to cellulose fibrillar networks. *Nature Communications*, 11(1), 4692.
- Bertasius, P., Macutkevics, J., Banys, J., Gaidukovs, S., Barkane, A., & Vaivodiss, R. (2020). Synergy effects in dielectric and thermal properties of layered ethylene vinyl acetate composites with carbon and Fe3O4 nanoparticles. *Journal of Applied Polymer Science*, 137(24), 48814.
- Brillard, A., Habermacher, D., & Brihac, J. F. (2017). Thermal degradations of used cotton fabrics and of cellulose: Kinetic and heat transfer modeling. *Cellulose*, 24(3), 1579–1595.
- Diaz, J. A., Ye, Z., Wu, X., Moore, A. L., Moon, R. J., Martini, A., et al. (2014). Thermal conductivity in nanostructured films: From single cellulose nanocrystals to bulk films. *Biomacromolecules*, 15(11), 4096–4101.
- Filipova, I., Serra, F., Tarrés, Q., Mutjé, P., & Delgado-Aguilar, M. (2020). Oxidative treatments for cellulose nanofibers production: A comparative study between TEMPO-mediated and ammonium persulfate oxidation. *Cellulose*, 27(18), 10671–10688.
- Gaidukovs, S., Zukulis, E., Bochkov, I., Vaivodiss, R., & Gaidukova, G. (2018). Enhanced mechanical, conductivity, and dielectric characteristics of ethylene vinyl acetate

- copolymer composite filled with carbon nanotubes. *Journal of Thermoplastic Composite Materials*, 31(9), 1161–1180.
- Goksu, E. I., Karamanlioglu, M., Bakir, U., Yilmaz, L., & Yilmazer, U. (2007). Production and characterization of films from cotton stalk xylan. *Journal of Agricultural and Food Chemistry*, 55(26), 10685–10691.
- Grantham, N. J., Wurman-Rodrich, J., Terrett, O. M., Lyczakowski, J. J., Stott, K., Iuga, D., et al. (2017). An even pattern of xylan substitution is critical for interaction with cellulose in plant cell walls. *Nature Plants*, 3(11), 859–865.
- Hanhikoski, S., Solala, I., Lahtinen, P., Niemelä, K., & Vuorinen, T. (2020). Fibrillation and characterization of lignin-containing neutral sulphite (NS) pulps rich in hemicelluloses and anionic charge. *Cellulose*, 27(12), 7203–7214.
- Hansen, N. M. L., Blomfeldt, T. O. J., Hedenqvist, M. S., & Plackett, D. V. (2012). Properties of plasticized composite films prepared from nanofibrillated cellulose and birch wood xylan. *Cellulose*, 19(6), 2015–2031.
- Henriksson, M., Berglund, L. A., Isaksson, P., Lindström, T., & Nishino, T. (2008). Cellulose nanopaper structures of high toughness. *Biomacromolecules*, 9(6), 1579–1585.
- Hubbe, M. A., Tayeb, P., Joyce, M., Tyagi, P., Kehoe, M., Dimic-Misic, K., & Pal, L. (2017). Rheology of nanocellulose-rich aqueous suspensions: A review. *BioResources*, 12(4), 106.
- Mahendra, I. P., Wirjosentono, B., Tamrin, Ismail H., & Mendez, J. A. (2019). Thermal and morphology properties of cellulose nanofiber from TEMPO-oxidized lower part of empty fruit bunches (LEFB). *Open Chemistry*, 17(1), 526–536.
- Ibrahim, N. A., Eid, B. M., El-Zairy, E. M., Emam, E., & Barakat, S. (2019). Environmentally sound approach for imparting antibacterial and UV-protection functionalities to linen cellulose using ascorbic acid. *International Journal of Biological Macromolecules*, 135, 88–96.
- Isaac, A., de Paula, J., Viana, C. M., Henriques, A. B., Malachias, A., & Montoro, L. A. (2018). From nano- to micrometer scale: The role of microwave-assisted acid and alkali pretreatments in the sugarcane biomass structure. *Biotechnology for Biofuels*, 11, 73.
- Isobe, N., Kasuga, T., & Nogi, M. (2018). Clear transparent cellulose nanopaper prepared from a concentrated dispersion by high-humidity drying. *RSC Advances*, 8(4), 1833–1837.
- Kumar, V., Pathak, P., & Bhardwaj, N. K. (2020). Waste paper: An underutilized but promising source for nanocellulose mining. *Waste Management*, 102, 281–303.
- Linder, Å., Bergman, R., Bodin, A., & Gatenholm, P. (2003). Mechanism of assembly of xylan onto cellulose surfaces. *Langmuir*, 19(12), 5072–5077.
- Liu, L., Cui, B., Tan, L., & Wang, W. (2021). Improving the combination of cellulose and lignin using xylan as a compatibilizer. *Cellulose*, 28(9), 5335–5349.
- Machado, G., Santos, F., Lourega, R., Mattia, J., Faria, D., Eichler, P., & Auler, A. (2020). *Biopolymers from Lignocellulosic Biomass* (pp. 125–158). Lignocellulosic Biorefining Technologies.
- Markstedt, K., Håkansson, K., Toriz, G., & Gatenholm, P. (2019). Materials from trees assembled by 3D printing – wood tissue beyond nature limits. *Applied Materials Today*, 15, 280–285.
- Martínez, Á. T., Speranza, M., Ruiz-Dueñas, F. J., Ferreira, P., Camarero, S., Guille n, F., et al. (2005). Biodegradation of lignocelluloses: Microbial, chemical, and enzymatic aspects of the fungal attack of lignin. *International Microbiology: The Official Journal of the Spanish Society for Microbiology*, 8(3), 195–204.
- Mtibe, A., Linganiso, L. Z., Mathew, A. P., Oksman, K., John, M. J., & Anandjiwala, R. D. (2015). A comparative study on properties of micro and nanopapers produced from cellulose and cellulose nanofibres. *Carbohydrate Polymers*, 118, 1–8.
- Naidu, D. S., Hlangothi, S. P., & John, M. J. (2018). Bio-based products from xylan: a review. *Carbohydrate Polymers*, 179, 28–41.
- Nunna, S., Chandra, P. R., Shrivastava, S., & Jalan, A. (2012). A review on mechanical behavior of natural fiber based hybrid composites. *Journal of Reinforced Plastics and Composites*, 31(11), 759–769.
- Rajinipriya, M., Nagalakshmaiah, M., Robert, M., & Elkoun, S. (2018). Importance of agricultural and industrial waste in the field of nanocellulose and recent industrial developments of wood based nanocellulose: A review. *ACS Sustainable Chemistry & Engineering*, 6(3), 2807–2828.
- Robles, E., Izaguirre, N., Martin, A., Moschou, D., & Labidi, J. (2021). Assessment of bleached and unbleached nanofibers from pistachio shells for nanopaper making. *Molecules*, 26(5), 1371.
- Sethi, J., Visanko, M., Osterberg, M., & Sirvio, J. A. (2019). A fast method to prepare mechanically strong and water resistant lignocellulosic nanopapers. *Carbohydrate Polymers*, 203, 148–156.
- Shen, D., Ye, J., Xiao, R., & Zhang, H. (2013). TG-MS analysis for thermal decomposition of cellulose under different atmospheres. *Carbohydrate Polymers*, 98(1), 514–521.
- Shen, D., Zhang, L., Xue, J., Guan, S., Liu, Q., & Xiao, R. (2015). Thermal degradation of xylan-based hemicellulose under oxidative atmosphere. *Carbohydrate Polymers*, 127, 363–371.
- Sun, J., Huang, J., E, L., Ma, C., Wu, Z., Xu, Z., et al. (2020). Wood-inspired compressible, mesoporous, and multifunctional carbon aerogel by a dual-activation strategy from cellulose. *ACS Sustainable Chemistry & Engineering*, 8(30), 11114–11122.
- Taylor, L., Phipps, J., Blackburn, S., Greenwood, R., & Skuse, D. (2020). Using fibre property measurements to predict the tensile index of microfibrillated cellulose nanopaper. *Cellulose*, 27(11), 6149–6162.
- Tedeschi, G., Guzman-Puyol, S., Ceseracciu, L., Paul, U. C., Picone, P., Di Carlo, M., et al. (2020). Multifunctional bioplastics inspired by wood composition: effect of hydrolyzed lignin addition to xylan–cellulose matrices. *Biomacromolecules*, 21(2), 910–920.
- Uetani, K., & Hatori, K. (2017). Thermal conductivity analysis and applications of nanocellulose materials. *Science and Technology of Advanced Materials*, 18(1), 877–892.
- Wang, J., Kasuya, K., Koga, H., Nogi, M., & Uetani, K. (2021). Thermal conductivity analysis of chitin and deacetylated-chitin nanofiber films under dry conditions. *Nanomaterials*, 11(3), 658.
- Watkins, D., Nuruddin, M., Hosur, M., Tcherbi-Narteh, A., & Jeelani, S. (2015). Extraction and characterization of lignin from different biomass resources. *Journal of Materials Research and Technology*, 4(1), 26–32.
- Xiao, S., Gao, R., Lu, Y., Li, J., & Sun, Q. (2015). Fabrication and characterization of nanofibrillated cellulose and its aerogels from natural pine needles. *Carbohydrate Polymers*, 119, 202–209.
- Zhang, C., Chen, G., Wang, X., Zhou, S., Yu, J., Feng, X., et al. (2020). Eco-friendly bioinspired interface design for high-performance cellulose nanofibril/carbon nanotube nanocomposites. *ACS Applied Materials & Interfaces*, 12(49), 55527–55535.
- Zhang, K., Sun, P., Liu, H., Shang, S., Song, J., & Wang, D. (2016). Extraction and comparison of carboxylated cellulose nanocrystals from bleached sugarcane bagasse pulp using two different oxidation methods. *Carbohydrate Polymers*, 138, 237–243.
- Zhang, N., Tao, P., Lu, Y., & Nie, S. (2019). Effect of lignin on the thermal stability of cellulose nanofibrils produced from bagasse pulp. *Cellulose*, 26(13-14), 7823–7835.